Published in final edited form as:
Traffic. 2009 October ; 10(10): 1488–1501. doi:10.1111/j.1600-0854.2009.00961.x.

Transferrin-directed Internalization and Cycling of Transferrin Receptor 2

Juxing Chen, **Jinzhi Wang**, **Kathrin R. Meyers**, and **Caroline A. Enns**[†]
Department of Cell and Developmental Biology L215, Oregon Health & Science University, Portland, OR 97239

Abstract

Transferrin receptor 2 (TfR2) is a homologue of transferrin receptor 1 (TfR1) but has distinct functions from TfR1 in iron homeostasis. In keeping with its proposed role in iron sensing, previous studies showed that TfR2 has a short half-life and that holo-Tf stabilizes TfR2 by redirecting it from a degradative pathway to a recycling pathway. In this study, we characterized how the endocytosis, recycling and degradation of TfR2 relates to its function and differs from TfR1. TfR2 endocytosis was AP-2-dependent. Flow cytometry analysis showed that TfR1 and TfR2 utilized the same endocytic pathway only in the presence of holo-Tf, indicating that holo-Tf alters the interaction of TfR2 with the endocytic machinery. Unlike TfR1, PACS-1 binds to the cytoplasmic domain of TfR2 and data suggest that PACS-1 is involved in the TfR2 recycling. Depletion of TSG101 by siRNA or expression of a dominant negative Vps4 inhibited TfR2 degradation, indicating that TfR2 degradation occurs through a multivesicular body (MVB) pathway. TfR2 degradation is not mediated through ubiquitination on the single lysine (K31) in the cytoplasmic domain or on the amino terminal residue. No ubiquitination of TfR2 by HA-ubiquitin was detected, indicating a lack direct TfR2 ubiquitination involvement in its degradation.

Keywords

TfR2; endocytosis; recycling; MVB; membrane protein degradation; hereditary hemochromatosis

Introduction

Transferrin receptor 2 (TfR2) plays an important role in iron homeostasis in the body. It is predominantly expressed in hepatocytes in the liver. The liver is a key organ in the regulation of iron levels. Disease-causing mutations in TfR2 or lack of TfR2 in humans and mice result in a form of hereditary hemochromatosis (HH). In HH, too much iron is taken up into the body resulting in cirrhosis of the liver, heart arrythmias, arthritis and diabetes due to iron overloading of these organs. The details of how TfR2 functions to maintain iron homeostasis are largely undefined. Recent evidence points to a role for TfR2 in sensing iron-laden Tf (holo-Tf) in the blood and stimulating the transcription of hepcidin, a peptide hormone secreted by hepatocytes (1). Hepcidin down-regulates the iron transporter, ferroportin (2). In the intestine ferroportin is responsible for the efflux of iron out of the intestinal epithelial cells into the rest of the body. TfR2 is postulated to maintain iron homeostasis in the body by sensing the level of holo-Tf in the blood, and transmitting a signal to positively regulate hepcidin expression. Thus high levels of holo-Tf stimulate hepcidin expression which down-regulates ferroportin and limit further iron uptake into the body.

[†]**Corresponding author**: Caroline A. Enns, Ph.D., Fax: (503) 494-4253, ennsca@ohsu.edu.

The level of TfR2 in the liver is regulated by an unusual post-translational mechanism, involving the stabilization of receptor upon binding to its ligand, holo-Tf (3–5). In the presence of high concentrations of holo-Tf in the blood, TfR2 is stabilized and presumably is able to signal longer to increase hepcidin transcription. Conversely, when the body is depleted of iron, serum levels of holo-Tf decline, TfR2 is rapidly degraded and no longer induces hepcidin expression.

The mechanisms by which TfR2 traffics, is stabilized by Tf, and is degraded within cells are less understood. Even though TfR2 is a homolog of the ubiquitous transferrin receptor 1 (TfR1) and the sequence of their ectodomains is 45% identical, the cytoplasmic domains bear no sequence similarity except for a YxxΦ internalization motif. TfR2 traffics differently than TfR1 in that a lysosomal process rapidly degrades TfR2 (6), whereas TfR1 continuously recycles to the cell surface and has a much longer half-life (7). The binding of Tf to TfR2 redirects TfR2 to a recycling pathway, which increases its lifetime in cells (6). Generation of TfR2/TfR1 chimeras indicates that the cytoplasmic domain of TfR2 is largely responsible for its rapid degradation (5). The addition of holo-Tf to cells expressing the TfR2/TfR1 chimera, containing only the cytoplasmic domain of TfR2, stabilizes the chimera to a similar extent as the addition of holo-Tf to cells expressing wild-type TfR2. These results demonstrate the importance of the TfR2 cytoplasmic domain in the Tf-dependent trafficking of TfR2.

In this study, we investigated the endocytosis, recycling and degradation of TfR2. The trafficking of TfR2 differs substantially than the trafficking of TfR1 in keeping with their different functions: TfR2 in maintaining iron homeostasis in the body vs TfR1 in maintaining cellular iron homostasis. Notably, we found that TfR2 and TfR1 did not compete for endocytosis in the absence of holo-Tf but did compete in the presence of holo-Tf, which implies that different mechanisms are involved in the internalization of unbound versus holo-Tf bound TfR2. Like TfR1, the endocytosis of TfR2 is AP-2 dependent, indicating that both receptors internalize by clathrin-mediated endocytosis. TfR2 but not TfR1 interacts with the sorting molecule phosphofurin acidic cluster sorting protein 1 (PACS-1), and our data suggest that the interaction between TfR2 and PACS-1 mediates recycling of TfR2 back to the cell surface. Finally, we established that the sorting of TfR2 to lysosomes for degradation most likely goes through a TSG101- and Vps4-mediated MVB pathway, and does not require direct ubiquitination of TfR2.

Results

TfR2 endocytosis is AP-2-dependent

The YxxΦ motif is important for the endocytosis of both TfR1 (8) and TfR2 (6). However, TfR2 and TfR1 only partially co-localize in Hep3B/TfR2 and HepG2 cells (6). Their common ligand, holo-Tf, traffics to late endosomal compartments in HeLa cells transfected with TfR2 but not in untransfected cells expressing endogenous TfR1 alone (9), implying that there are distinct roles for TfR2 and TfR1 in sequestration of Tf. In addition, holo-Tf redirects the trafficking of TfR2 from a degradative pathway to a recycling pathway (6), although it does not affect the trafficking of TfR1, which internalizes constitutively with or without Tf (10) by an AP-2-dependent mechanism (11).

Since TfR2 has an YxxΦ endocytic motif and mutation of Y23 to A in this motif inhibits its endocytosis (6), we tested whether TfR2 internalization was mediated by AP-2. If this were the case, then more TfR2 would be on the cell surface when clathrin-mediated endocytosis is inhibited. Depletion of the μ2 subunit of AP-2 by siRNA reduces levels of other subunits by decreasing the overall complex stability (11). HeLa/tTA-TfR2 cells, which express endogenous TfR1 and exogenous TfR2 that can be repressed with addition of dox, were

used in these experiments. The μ2 subunit of AP-2 was depleted with siRNA, and surface levels of TfR2 were measured by flow cytometry. TfR1 was used as a positive control. We observed that when the μ2 subunit of AP-2 was depleted by siRNA (Figure 1A), surface TfR2 and TfR1 levels increased by 1.62 and 2.28 fold, respectively (Figure 1B). This result suggested that depletion of AP-2 disrupted endocytosis of TfR2 as well as TfR1. Since blocking internalization also blocks lysosomal degradation, a slight increase of total TfR2 and TfR1 levels was observed in AP-2 depleted cells (Figure 1A). To confirm the dependence of TfR2 endocytosis on AP-2, the uptake of holo-bovine-Tf^{-488} (300 nM), which binds to TfR2 but not to TfR1 (7), was examined by confocal microscopy. Holo-bovine Tf^{-488} was internalized in the control siRNA-treated cells but remained on the cell surface in the μ2 siRNA-treated cells (Figure 1C). The endocytosis of TfR1 was monitored to ensure sufficient depletion of μ2 to block endocytosis. Consistent with previous results that TfR1 endocytosis requires the μ2 subunit of AP-2 (11), the holo human-Tf^{594} (holo-Tf^{594}), which binds to TfR1, remained on cell surface in HeLa/tTA-TfR2 cells upon depletion of the μ2 subunit of AP-2 and repression of TfR2 expression (Figure 1D). To further confirm these results, we measured the uptake of ^{125}I-holo-bovine Tf and ^{125}I-holo-Tf in AP-2-depleted cells. The internalized to surface ratio of ^{125}I-holo-bovine Tf and ^{125}I-holo-Tf significantly decreased by 57.2% and 70.8% respectively in response to knockdown of μ2 AP-2 (Figure 1E). These results indicated that TfR2-mediated endocytosis of holo bovine-Tf and TfR1-mediated endocytosis of holo-Tf are both dependent on AP-2. Consistent with these results, the ratio of internalized to surface ^{125}I-holo-bovine Tf (1.23) and ^{125}I-holo-Tf (0.91) in control cells was similar to the ratio of intracellular to surface levels of TfR2 and TfR1 (1.27 and 1.30) that were measured in steady state by flow cytometry (Figure 1F). Taken together, these experiments demonstrated that TfR2 endocytosis, like TfR1 endocytosis, is dependent on AP-2.

TfR2 and TfR1 use similar mechanisms for endocytosis only in the presence of holo-Tf

Since both TfR2 and TfR1 have YxxΦ motif and their endocytosis is dependent on AP-2, we tested whether they internalize by similar mechanisms using a competition assay that was used by Marks and colleagues (12). In this approach, if the two receptors compete for endocytosis, over-expression of one receptor will saturate its endocytic pathway, therefore inhibit endocytosis of another receptor, which would cause this receptor redistributed to cell surface (12–14). HeLa/tTA-TfR2 cells, in which TfR2 expression can be turned off by adding 1 μg/ml of dox for 5 days (Figure 2A), were used to address this issue. Because TfR1 is negatively regulated by intracellular iron concentrations, over-expression of TfR2 would bring more iron into the cells, which would lead to a decrease in the total amount of TfR1. To eliminate this effect, an iron chelator, deferoxamine (150 μM), was added to cells for 1 day prior to the experiment to deplete iron, which would then up-regulate TfR1 expression to a high and constant level shown in Figure 2A. A constant level of TfR1 is important for detection of any change in distribution (surface to total (S/T) ratio) of TfR1. Flow cytometry analysis showed that increased expression of TfR2 (Figure 2A) did not significantly alter S/T ratio of TfR1 (Figure 2B), indicating that up-regulation of TfR2 did not inhibit TfR1 internalization.

The differences in endocytosis of TfR2 and TfR1 in the absence of holo-Tf were verified by measuring the competition between the two Tf receptors and Lamp1, because of this unusual finding. TfR1 competes with Lamp1 for endocytosis. Over-expression of TfR1 causes the redistribution of Lamp1 to the cell surface, which indicates that they use the same connector molecules for endocytosis (13). If TfR2 does not compete with TfR1 for endocytosis, then TfR2 should not compete with Lamp1 either. HeLa/TfR1 20-2 cells in which TfR1 can be over-expressed in the absence of dox, were used in this experiment (13). Surface TfR1 and Lamp1 levels were analyzed in the absence of dox. In addition, surface TfR2 and Lamp1

levels were analyzed in HeLa/TfR1 cells transiently transfected with TfR2 and grown in the presence of dox, which was used to decrease TfR1 expression to endogenous levels. As predicted, TfR1 and Lamp1 competed for endocytosis as determined by increased surface Lamp1 levels with increased TfR1 expression (Figure 2C). However, the amount of Lamp1 on the cell surface did not increase with increasing amounts of TfR2 (Figure 2D), indicating that TfR2 did not compete with Lamp1 for endocytosis.

These results indicate that TfR2 and TfR1 do not compete for endocytosis in the absence of added holo-Tf, and suggest two possibilities: TfR1 and TfR2 could either interact with different connector molecules for endocytosis or internalize through distinct AP-2 vesicles.

The ability of TfR2 and TfR1 to compete with each other for endocytosis in the presence of saturating amounts of holo-Tf was tested in cells overexpressing TfR2. Hela/tTA-TfR2 cells were treated with 25 μM human holo-Tf (holo-Tf) for 30 min at 37°C. Surface and total levels of TfR2 and TfR1 were measured by flow cytometry. In the presence of holo-Tf, S/T ratio of TfR1 significantly increased by 28% when TfR2 was expressed (Figure 2B), suggesting that over-expression of TfR2 results in the redistribution of TfR1 to the cell surface. Thus, TfR2 and TfR1 competed with each other for endocytosis in the presence of holo-Tf. Because holo-Tf binds to both TfR1 and TfR2, we tested whether the competition of endocytosis between TfR2 and TfR1 was caused by the binding of holo-Tf to TfR2 or TfR1 or both. Cells were treated with holo-bovine Tf, which binds to TfR2 but not detectably to TfR1 (7), and the surface and total levels of TfR1 were measured by flow cytometry. Like treatment with human holo-Tf, the S/T ratio of TfR1 increased by 32%, in response to holo-bovine Tf treatment (Figure 2B), suggesting that the binding of Tf to TfR2 is sufficient to redirect the endocytosis of TfR2 to the same pathway used by TfR1.

PACS-1 depletion alters the trafficking of TfR2 but not TfR1

The cytoplasmic domain of TfR2 is largely responsible for Tf-sensitive stabilization (5). However, the motif responsible for the altered trafficking of TfR2 and the proteins that mediate this pathway are still unknown. Sequence analysis of the cytoplasmic domain of all mammalian TfR2 proteins revealed a highly conserved acidic cluster motif (EEEEEDGEEGAE) (Figure 3A), which is a potential PACS-1 binding site. PACS-1 is a cytosolic molecule that directs the sorting of membrane proteins containing an acidic cluster-sorting motif in the trans-Golgi network (TGN) and the endosomal system (15,16). Hep3B/TfR2 cells, which express both TfR1 and TfR2, were infected with PACS-1-HA adenovirus, in order to test whether TfR2 interacts with PACS-1. Cell lysates were immunoprecipitated with an anti-HA antibody. The immunoprecipitated proteins were detected with rabbit anti-TfR2 and mouse anti-TfR1 antibodies. PACS-1-HA interacted with TfR2 but not with TfR1 (Figure 3B), which contains a much shorter acid cluster motif (DEEE) (Figure 3A). The interaction of TfR2 but not TfR1 with PACS-1-HA was also detected in reciprocal immunoprecipitation with anti-TfR2 and anti-TfR1 antibodies, respectively, followed by immunodetection with anti-HA antibody (data not shown). Moreover, endogenous TfR2 interacted with endogenous PACS-1 in HepG2 cells, and the presence of holo-Tf did not abrogate the interaction (Figure 3C). A mutant TfR2, ΔE-TfR2, lacking the acidic cluster motif was constructed by site-directed mutagenesis and then transfected into Hep3B cells to generate a stable cell line, Hep3B/ΔE-TfR2 to test if the acidic cluster motif is necessary for the interaction between TfR2 and PACS-1. In contrast to wt-TfR2, ΔE-TfR2 did not interact with PACS-1 by immunoprecipitation with rabbit anti-TfR2 antibody (Figure 3D). This result indicated that the acidic cluster motif is essential for the binding of TfR2 to PACS-1.

We wanted to determine the function of PACS-1 in the regulation and trafficking of TfR2, since PACS-1 interacted with TfR2 but not with TfR1. Hep3B/TfR2 cells were transfected

with PACS-1 specific or control siRNA for 32 hr, and then treated with holo-Tf for 24 hr. Cell lysates were analyzed by immunoblot. Knockdown of PACS-1 had no effect on the total levels of TfR2 and TfR1 or on the stabilization of TfR2 by holo-Tf (Figure 3E). Thus PACS-1 is not involved in the Tf-sensitive rerouting of TfR2 from a degradative pathway to a recycling pathway.

To examine whether PACS-1 alters the distribution of TfR2, surface and total levels of TfR2 and TfR1 were measured by flow cytometry. Knockdown of PACS-1 decreased TfR2 surface levels (Figure 3F) and S/T ratio (Figure 3G) by 35% and 48%, respectively. Consistent with the immunoblot results (Figure 3E), total TfR2 and TfR1 levels did not change significantly after depletion of PACS-1 (Figure 3F). The S/T ratio of TfR1 did not change significantly (Figure 3G) because TfR1 did not interact with PACS-1 (Figure 3B).

The decrease of TfR2 S/T ratio in PACS-1-depleted cells suggests that PACS-1 functions either in decreasing TfR2 internalization or increasing TfR2 recycling. To distinguish between these possibilities, internalization of TfR2 was measured by biotinylation. Cells were cooled on ice and cell surface proteins were biotinylated with sulfo-NHS-SS-biotin for 20 mins. Biotinylated cells were then warmed to 37°C for 0–10 min. At the indicated time, they were again cooled on ice and any remaining biotin on the cell surface was removed with MesNa, an impermeable reducing agent. Internalized biotinylated proteins were isolated with streptavidin-coupled beads and TfR2 was quantified by immunoblot analysis. TfR2 was internalized at a similar rate in the control and PACS-1-depleted cells (Figure 3J, K). In addition, the degradation rate of TfR2 was not affected by the depletion of PACS-1 (Figure 3H, I). Although we could not directly measure recycling rate of TfR2, our findings that depletion of PACS-1 decreased cell surface TfR2 levels but did not change total TfR2 levels or alter the internalization and degradation rate of TfR2, suggest that repression of PACS-1 slows down TfR2 recycling rather than increases its endocytosis.

Depletion of PACS-1 resulted in less TfR2 on the cell surface and therefore a greater amount of intracellular TfR2. To identify the intracellular compartment(s) that contain TfR2, co-localization of TfR2 with TfR1 (early/recycling endosome marker), EEA1 (early endosome marker) and AP-1 (endosome and Golgi marker) was measured by quantitative co-localization analysis as described previously (6). The fraction of TfR2 that co-localized with EEA1 and TfR1 increased by 32.2% and 35.0%, respectively, in PACS-1-depleted cells, but the small fraction of TfR2 that co-localized with AP-1 was not significantly affected (Figure 3L). Taken together, these data suggest that PACS-1 promotes the recycling of TfR2 from early endosome and recycling endosome compartments to the cell surface.

TfR2 is degraded in the lysosome most likely through the MVB pathway

TfR2 is degraded in the lysosome (6); however, the exact pathway of TfR2 targeting to the lysosome remains unclear. A key step in late endosomal sorting is the formation of the multivesicular body (MVB), in which the endosomal membrane invaginates to form intralumenal vesicle (ILV). Many membrane proteins destined for lysosome degradation are sorted to these vesicles prior to degradation, most of which is mediated by their ubiquitination (17,18). Specifically, the membrane proteins are ubiquitinated, recruited by Hrs, concentrated in clathrin-coated membranes of sorting endosome, and incorporated into an inwardly budding vesicle in the presence of TSG101, a homologue of Vps23 and a core component of endosomal sorting complex required for transport (ESCRT)-I. ESCRT-I activates ESCRT-II, which then recruits ESCRT-III at the endosome. Finally, Vps4, an ATPase of the AAA protein family, dissociates ESCRT complex and releases cargo proteins, and fission occurs to produce MVBs. Fusion of MVBs with lysosomes results in degradation of the proteins within the MVB (19,20).

Two approaches were used to test whether TfR2 trafficked through this pathway. First TSG101, which binds ubiquitinated membrane cargos and plays an essential role in their lysosomal/vacuolar sorting and MVB formation (21), was suppressed by siRNA in Hep3B/TfR2 cells. The cells endogenously express EGF receptor (EGFR). EGFR traffics through the MVB pathway for degradation and its degradation is blocked by knockdown of TSG101 (22), therefore EFGR was used as a positive control for TSG101 depletion. After transfection with TSG101 siRNA for 40 hr, cells were split to four wells and treated with or without 25 μM holo-Tf for 24 hr followed by serum starvation overnight to induce EGFR expression. One set of cells was then treated with 25 ng/ml EGF for 3 hr to induce EGFR degradation. EGF-stimulated EGFR degradation was quantitated to determine the extent to which the knockdown of TSG101 stabilizes EGFR. EGFR degradation was reduced but not eliminated by TSG101 siRNA (Figure 4A), perhaps because TSG101 was not totally depleted in our system. Similar to what was seen for EGFR, TfR2 levels increased by about 2.5 fold in TSG101-repressed cells when compared with the corresponding lanes in control siRNA treated cells, and this increase was holo-Tf independent; moreover, in response to holo-Tf treatment, TfR2 increased by 2–4.5 fold regardless of TSG101 repression (Figure 4A). If TSG101 were efficiently depleted, we would expect to see complete block of TfR2 degradation and no further response of TfR2 to holo-Tf.

Since repression of TSG101 increased the steady-state level of TfR2, we tested whether it blocked degradation of surface TfR2. The degradation rate of surface TfR2, which was labeled with biotin (Figure S1), was very similar to that of total TfR2 measured by cycloheximide (chx) treatment (Figure 3J). Therefore, control and TSG101-depleted cells were treated with chx to inhibit protein synthesis for 0–12 hr (Figure 4B). TfR2 degradation was significantly inhibited upon knockdown of TSG101, and TfR2 was further stabilized by holo-Tf in TSG101-depleted cells (Figure 4B), which is consistent with the steady state regulation of TfR2 by TSG101 (Figure 4A). In line with Figure 4A and previous finding that TfR2 is stabilized by holo-Tf (3, 4), TfR2 is more stable when the cells were treated with holo-Tf. The half-life of TfR2 in TSG101-depleted cells was 14 hr, which was 2.5 times longer than that in the control siRNA-treated cells (5.6 hr) and similar to that measured in the control cells treated with holo-Tf (12.7 hr), but shorter than that in TSG101-depleted cells upon treatment with holo-Tf, in which no significant decay of TfR2 was observed (Figure 4C). These results are presumably due to incomplete knockdown of TSG101 (Figure 4A). Taken together, knockdown of TSG101 inhibits TfR2 degradation, which is similar to what was observed for EGFR. Thus, like EGFR, TfR2 likely traffics through the MVB to the lysosome for degradation.

We then tested whether TfR2 accumulated in early endosomes upon TSG101 depletion, as does EGFR (22–25). The fraction of TfR2 co-localizing with the early endosome marker EEA1 and the recycling/early endosome marker TfR1 in the control and TSG101-depleted cells was quantified. The amount of TfR2 that co-localized with EEA1 increased by 20% in TSG101-depleted cells, but no significant change in the fraction of TfR2 that co-localized with TfR1 was observed (Figure 4D). Some tubular cluster structures in early endosomes were observed in TSG101-depleted cells but not in control cells (Figure 4E). This finding is similar to the observation that depletion of TSG101 leads early endosome to form enlarged tubular clusters in A431 cells (25). Depleting cells of TSG101 can have pleotropic effects such as blocking bulk flow to lysosomes and blocking recycling.

Secondly, to further test whether TfR2 is degraded through a MVB pathway, a later step in MVB formation was blocked. A dominant negative mutant of Vps4, GFP-Vps4$_{R228Q}$, which blocks ATP hydrolysis, and wild-type GFP-Vps4 as a control, were transiently transfected into Hep3B/TfR2 cells for 15 hr followed by treatment with holo-Tf. Similar to the depletion of TSG101, TfR2 levels increased by about 3.5 fold after transfection of GFP-Vps4$_{R228Q}$,

and only increased by 1.4 fold after transfection with wild-type GFP-Vps4 (Figure 4F, Figure S2). The wild-type Vps4 was used because over expression of Vps4 can inhibit the formation of MVBs, but to a much lower extent than the dominant negative constructs (26). All forms of GFP-VPS4 were expressed at similar levels (Figure S2). These results indicated that a dominant negative mutant of Vps4, which inhibits intralumenal vesicle formation, inhibited TfR2 degradation. The results that depletion of TSG101 and expression of dominant negative Vps4 both inhibited degradation of TfR2 indicate that TfR2 is targeted to MVB prior to degradation.

Lack of detectable TfR2 ubiquitination along the degradative pathway

Ubiquitin modification is a major signal for cargo membrane proteins that traffic to the lysosome for degradation through MVB pathway. To determine whether TfR2 entry into MVB pathway requires ubiquitination, we mutated the only lysine (K) in its cytoplasmic domain, K31, to an alanine (A). If ubiquitination of K31 is involved in TfR2 degradation, the K31A mutant TfR2 would not be ubiquitinated and therefore would be more stable than wild type TfR2 and not respond to knockdown of TSG101. To test if this was the case, TSG101 was repressed by specific siRNA in Hep3B/K31A-TfR2 cells. Like wild type TfR2 (Figure 4A), K31A-TfR2 levels increased by 2.7 fold and still responded to holo-Tf treatment upon depletion of TSG101 (Figure 5A). Consistent with the lack of involvement of K31 in the degradation of TfR2, the half-life of K31A-TfR2 was similar to wild type TfR2 and increased by 1.8 fold when the cells were treated with holo-Tf (Supplemental Table 1). These results suggested that TfR2 is targeted to the MVB independently of possible ubiquitin modification of K31.

TfR2 is a type II membrane protein with its N-terminus facing the cytoplasm, presenting the possibility that TfR2 could be ubiquitinated on the α-NH2 of N-terminal residue. A number of proteins such as MyoD, E7, LMP1, LMP2A, Id2 and p21 are modified in this way (27). GFP, fused to the N-terminus of proteins, has been used to block amino-terminal ubiquitination in several studies (27–30). Therefore, a GFP tag was fused to the N-terminus of TfR2 (GFP-TfR2) to test for this possibility. GFP-TfR2 was expressed in TRVb cells, which do not express endogenous TfR1 and therefore Tf only binds to TfR2. Holo-Tf^{594} uptake was performed to determine whether GFP-TfR2 is internalized. Holo-Tf^{594} was internalized as well as untagged TfR2 (Figure 1C) after incubation for 20 min at 37°C, and the internalized holo-Tf^{594} was largely co-localized with GFP (Figure 5B). GFP-TfR2 was also internalized in Hep3B/GFP-TfR2 cells in an anti-TfR2 monoclonal antibody uptake assay (Figure S3). Immunoblots (Figure 5C) showed that, similar to wild type TfR2, the level of GFP-TfR2 increased by about 3-fold with depletion of TSG101 in the presence or absence of holo-Tf. Interestingly, unlike wild type TfR2, GFP-TfR2 did not increase when the cells were treated with holo-Tf, irrespective of TSG101 knockdown. To confirm these results, the intensities of GFP-TfR2 were measured by flow cytometry after TSG101 depletion. Consistent with immunoblot results (Figure 5C), GFP-TfR2 increased by 2.6 fold in response to knockdown of TSG101, and was not further stabilized by holo-Tf (Figure 5D). Thus, TfR2 degradation was not mediated by the ubiquitination of the N-terminal methionine.

Some proteins like HLA-B7 and Bid can be ubiquitinated on amino acids other than the α-NH_2 of the N-terminus or lysine residues (31,32). To test for this possibility, HA-ubiquitin was co-transiently transfected with TfR2 at a ratio of 10:1 into Hep3B cells, and the possibility of TfR2 ubiquitination was determined by immunoprecipitation with anti-TfR2 antibody followed by immunoblot with anti-TfR2 and anti-HA antibodies to detect ubiquitinated species. As a positive control, GFPu, an enhanced GFP (EGFP) with 16-amino acid CL1 degron at its carboxy terminus to target it for polyubquitination (33), was used. HA-ubiquitin and GFPu were transiently co-transfected into Hep3B cells at a ratio of 10:1,

and GFPu was immunoprecipitated with rabbit anti-GFP antibody. No ubiquitinated forms of TfR2 were detected, although, polyubiquitinated species of GFPu were observed when HA-ubiquitin was expressed in the cells (Figure S4). These results suggested that unlike GFPu, TfR2 is not ubiquitinated by HA-ubiquitin. Taken together, these results indicate that TfR2 targeting to the MVB for degradation does not require direct ubiquitination.

Discussion

TfR2 differs from TfR1 in both its function and trafficking. TfR1 brings iron into cells by binding holo-Tf and internalizing via clathrin-coated vesicles and participates in the release of iron from Tf in acidic vesicles (34,35). In keeping with its function, TfR1 is expressed in most proliferating cells and is stable with a half-life of ~19–24 hr (36,37), and cycling many times before being degraded. TfR1 is negatively regulated by intracellular iron concentrations at the level of mRNA stability, which is consistent with its function in supplying cells with iron and regulating intracellular iron homeostasis. In contrast, TfR2 is involved in signaling as well as iron uptake (1). It is mainly expressed in hepatocytes where it participates in communicating holo-Tf levels in the blood to induce hepcidin synthesis. Increases in holo-Tf levels result in increased hepcidin transcription, which serves as a negative feedback mechanism to limit further uptake of iron by the body. The much shorter half-life of TfR2 and its regulation by holo-Tf reflects its function in maintaining iron homeostasis in the body. The half-life of TfR2 is about 4 hr in the absence of holo-Tf (3). Addition of holo-Tf over a physiological range levels increases the stability of TfR2 by 2~3 fold (3{Robb, 2004 #4944). We hypothesize that increasing the half-life of TfR2 with holo-Tf would allow the upregulation of hepcidin expression. Hepcidin negatively regulates iron uptake into the body. Therefore, iron homeostasis could be maintained through this feedback mechanism. Our previous studies indicated that both holo-Tf binding and the TfR2 cytoplasmic domain are critical for TfR2 stability and trafficking (5). Mutations in the ectodomain of TfR2 that abrogate Tf binding result in the rapid turnover of TfR2, lowering TfR2 levels and thus reducing its ability to signal (6). Substitution of TfR2 with the cytoplasmic domain of TfR1 results in a chimera that is not regulated by the addition of Tf (5). These results led us to examine the basis for the difference in the trafficking between TfR2 and TfR1.

In this study, we showed that, like TfR1, TfR2 endocytosis is AP-2-dependent. AP-2 is required for clathrin-mediated endocytosis (11,38). Depletion of the μ2 subunit of AP-2 resulted in the redistribution of TfR2 to cell surface and blocked TfR2-mediated holo-bovine Tf uptake. Thus the different functions of TfR1 and TfR2 are not due to the differences between clathrin and non-clathrin pathways of endocytosis. These results are in contrast to a previous report that TfR2 internalizes in a caveolin dependent manner (39). The basis for these differences is not entirely clear, but may be related to the antibodies used to detect TfR2. The monoclonal and polyclonal antibodies that we used were generated using a purified ectodomain of human TfR2. The molecular weight of the protein that is detected by Calzolari and colleagues differs from the molecular weight of TfR2 reported by us and other groups (40,41).

TfR1 and TfR2 do not compete for endocytosis in the absence of holo-Tf in HeLa cells, suggesting that although both receptors internalize by an AP-2-dependent pathway, they may interact with different accessory proteins that are involved in receptor-mediated endocytosis. TfR1 has been reported to interact with AP-2 directly (7,8) or be connected to AP-2 indirectly by TTP (42). Whether TfR2 directly interacts with AP-2 or through any other interacting partners is presently unknown. Since our results were obtained in a non-hepatic cell line, our data indicate that the difference in the endocytosis of TfR1 and TfR2 is not unique to hepatocytes. Interestingly, in the presence of holo-Tf or holo-bovine Tf, TfR2

and TfR1 compete with each other for endocytosis, suggesting that, unlike unbound TfR2, holo-Tf bound TfR2 is directed to use the same endocytic elements as TfR1. These results are consistent with our previous finding that holo-Tf redirects TfR2 from a degradative pathway to a recycling pathway (6), that is similar to constitutive recycling of TfR1 back to cell surface.

The fact that TfR2 uses two different pathways for endocytosis could be physiologically important. Other receptors are redirected to change the mode of endocytosis upon ligand binding. Nerve growth factor redirects p75NTR, the p75 neurotrophin receptor, from a rapid dynamin-dependent and clathrin-independent recycling process into clathrin-mediated endocytosis (43). BMP receptor type 2 (BRII) is internalized through both clathrin- and caveolae-mediated endocytic pathways; however, BMP receptor type 1(BRI) is only internalized through a clathrin-dependent pathway (44). Clathrin-mediated endocytosis of BMP receptors upon BMP-2 binding initiates Smad-dependent signaling, whereas caveolin-mediated internalization of BRII results in Smad-independent signaling (44). The mechanism by which the different internalization pathway of TfR2 initiated by holo-Tf affects hepcidin regulation remains to be determined.

Our data suggest that PACS-1 is involved in the trafficking of TfR2. PACS-1 is required for TGN localization of several membrane proteins containing an acid cluster motif, such as furin, CI-MPR, PC6B, VMAT-2 and HIV-1 viral protein, nef (15). It associates with the adaptor protein complex-1 (AP-1) and forms a ternary complex between furin and AP-1 (45,46). PACS-1 can also be involved in cycling furin to a plasma membrane-endosomal pathway. When furin is phosphorylated by casein kinase 2 (CKII), it is directed toward a cell surface-endosomal recycling pathway by virtue of its selective interaction with PACS-1 (47). In the case of TfR2, depletion of PACS-1 leads to less TfR2 on the cell surface and more TfR2 accumulation in intracellular compartments including early endosome (EEA1) and recycling endosome (TfR1), but it does not affect total levels of TfR2 or the rates of TfR2 internalization and degradation. These results suggest that PACS-1 functions mainly in the recycling of TfR2 back to the cell surface.

TSG101 and Vps4 are two critical proteins for early and late steps of MVB sorting pathway, respectively (21,48,49). Depletion of TSG101 or over-expression of a dominant negative VPS4 inhibited TfR2 degradation and suggests that TfR2 is likely degraded through MVB pathway. Tf endocytosed by TfR2 has been shown to localize in MVB by immunoelectron microscopy (9), which is consistent with our results that TfR2 is sorted to the lysosome for degradation by MVB pathway. Many membrane proteins require covalent modification by ubiquitin for entrance into the MVB pathway. Mutation of the only lysine in the cytoplasmic domain did not alter the inhibitory effect of TSG101 depletion on degradation of TfR2, demonstrating that TfR2 degradation does not occur via traditional lysine-mediated ubiquitination. Degradation of some proteins can also be mediated by the addition of ubiquitin to a nontraditional, non-lysine target residue. Degradation of the latent membrane protein 1 (LMP1) of the Epstein-Barr virus in immune-suppressed patients and the E7 human papillomavirus oncoprotein is dependent on ubiquitin and the proteasome but not on lysine residues, which indirectly indicates that a ubiquitin chain could be added to the N-terminal methionine residue (50–52). Bloom and colleagues showed direct proof that both wild type cyclin-dependent kinase inhibitor p21, and p21 (K0) mutant with all of its six lysines mutated to arginines are ubiquitinated at the N-terminus in vivo (28). However, this is not the case for TfR2, because disruption of the N-terminal α-NH_2 group by fusion of GFP does not affect the TSG101-mediated degradation of TfR2. Thus, direct ubiquitination of TfR2 is not required for its degradation.

Other proteins that undergo lysosomal degradation are independent of ubiquitination. The delta opioid receptor (DOR), a G protein-coupled receptor, undergoes agonist-induced ubiquitination-independent lysosomal degradation (53). The lysosomal trafficking of DOR is dependent on Hrs and Vps4/Skd1, which mediate very early and late steps, respectively, in lysosomal sorting of ubiquitinated cargo, but is not dependent on TSG101. Similar to DOR, TfR2 degradation does not need direct ubiquitination and require proper function of Vps4; in contrast, TfR2 degradation is also dependent on TSG101, whether it is laos dependent on Hrs remains to be determined. The melanosomal protein Pmel17 is targeted to ILVs of MVB for degradation, which is independent of ubiquitination, Hrs, TSG101 and Vps4 but requires sorting signal on its luminal domain (26). This case is not applicable for TfR2 since the cytoplasmic domain of TfR2 is largely responsible for its stabilization and TfR2 degradation requires TSG101 and Vps4. The sorting of Sna3p into the MVB pathway does not require ubiquitination, but it does require an N-terminal tyrosine (Y) containing sequence and a PPAY motif within its C-terminal cytosolic tail (29,30,54). TfR2 does not contain a PPAY motif but has a tyrosine (Y23) in its cytoplasmic domain. Since Y23 is required for endocytosis and mutation of the TfR2 Y23 to alanine blocks its internalization (6), we were not able to determine if it affects the sorting of TfR2 to MVBs.

Lack of detectable TfR2 ubiquitinatination by HA-ubiquitin indicates that TfR2 trafficking to the lysosome for degradation does not involve direct ubiquitination of TfR2. However, we cannot exclude that TfR2 may associate with a ubiquitinated protein, which would then direct TfR2 to the MVB. Tf binding may block this interaction, which would explain the Tf-mediated stabilization of TfR2. The protein (s) that direct TfR2 to the MVB pathway for degradation in the lysosome remains to be determined.

Materials and methods

Plasmid construction

The plasmids of pcDNA3/K31A-TfR2 and pcDNA3/ΔE-TfR2 (deletion of EEEEEDGEE) were generated by QuikChange XL site-directed mutagenesis (Strategene, La Jolla, CA) using pcDNA3/TfR2 (6) as template. The pcDNA3/GFP-TfR2 was generated by insertion of a GFP fragment to the N-terminus of TfR2. The pMT123/HA-ubiquitin and pEGFP-C1-GFPu plasmids were kindly provided by Dr. Linda Musil (Oregon Health & Science University (OHSU), Portland, Oregon). The plasmids of pEGFP-wt-VPS4 and pEGFP-R228Q-VPS4 were kindly provided by Dr. Wes Sundquist (University of Utah).

Antibodies

Rabbit anti-hTfR2 (16637) (3), mouse monoclonal anti-hTfR2 (9F8-1C11) (55) and mouse anti-TfR1 (3B82A1) (55) antibodies were described previously. Mouse anti-HA and anti-actin were purchased from Covance (California, CA) and Chemicon (Temecula, CA), respectively. Mouse anti-early endosome antigen 1 (EEA1), mouse anti-γ-adaptin (AP-1), anti-μ2-AP-2 (AP.50), and anti-α-AP-2 (AP.6) antibodies were purchased from Abcam (Cambridge, United Kingdom), Sigma-Aldrich (St. Louis, MO), BD Bioscience Pharmingen (San Diego, CA) and Calbiochem (La Jolla, CA), respectively. Mouse anti-TSG101 antibody (GeneTex, San Antonio, TX, USA) was kindly provided by Dr. Jerry Kaplan (The University of Utah, Salt Lake City, Utah). Rabbit anti-GFP (ab6556-25) was purchased from Abcam (Cambridge, MA). Rabbit anti-PACS-1 703 antibody (56) was kindly provided by Dr. Gary Thomas (OHSU). Mouse anti-GFP antibody (632381) from Clontech (Palo Alto, CA) was kindly provided by Dr. Linda Musil. Secondary antibodies against rabbit and mouse IgG conjugated to horseradish peroxidase (HRP) were purchased from Chemicon. Fluorescence-labeled Alexa 680 goat anti-rabbit IgG and Alexa 546 rabbit anti-mouse IgG

were purchased from Molecular Probes (Eugene, OR). IRDye 800 donkey anti-mouse IgG secondary antibody was purchased from Rockland Immunochemicals (Gilbertsville, PA).

Cell culture, transfection and generation of stable cell lines

Hep3B and HepG2 cells were maintained in Minimum Essential Medium Eagle (MEM) (Life Technologies, Bethesda, MD) supplemented with 1.0 mM sodium pyruvate, 0.1 mM nonessential amino acids (Life Technologies), and 10% fetal bovine serum (FBS). Hep3B cells were transfected with the pcDNA3/ΔE-TfR2, pcDNA3/K31A-TfR2 or pcDNA3-GFP-TfR2 plasmid (6) using Lipofectamine (Invitrogen, Carlsbad, CA) and selected with 400 μg/ml G418 as described previously (5) to generate Hep3B/ΔE-TfR2, and Hep3B/K31A-TfR2, and Hep3B/GFP-TfR2 cell lines, which were maintained in the above medium with addition of 400 μg/ml G418. The plasmids of pEGFP-wt-VPS4 and pEGFP-R228Q-VPS4 were transfected into Hep3B/TfR2 cells in 35-mm plates using 1 μg plasmid/5 μl Fugene HD (Roche Diagnostic, Indianapolis, IN).

Immunoprecipitation

Hep3B/TfR2 cells grown to 80% confluence were infected with adenovirus expressing PACS-1 (m.o.i.10) and trans adenovirus (m.o.i. 5) for 40 hr. Cells were lysed on ice in NET/T buffer (150 mM NaCl, 5 mM EDTA, 10 mM Tris, pH 7.4, 1% Triton X-100) containing 1× Complete Mini Protease Inhibitor Cocktail (Roche Diagnostic, Indianapolis, IN). Cell lysates were cleared by centrifugation at 15,000 × g for 10 min. Hep3B or Hep3B/TfR2 cells grown to 70% confluence were transfected with plasmid as described in the figure legends for 48 hr, and cells were lysed as described above. Protein concentration was measured using the BCA Protein Assay (Pierce, Rockford, IL). Lysates (50–200 μg total proteins) were pre-cleared with either Sepharose-4B/Protein A (Zymed, San Francisco, CA) or immobilized Protein G (Pierce), Rockford, IL) beads for 60 min at 4°C. The pre-cleared lysates were rotated overnight at 4°C with antibodies, and incubated with either Sepharose-4B/Protein A or immobilized Protein G for 2 hr. After centrifugation, the beads were washed three times with NET/T buffer, and the proteins were eluted with 2 × Laemmli buffer (57) and denatured by heating at 95 °C for 5 mins before loading on SDS polyacrylamide gel electrophoresis (SDS-PAGE) gel. All samples were subjected to 8%, 10% or 12% SDS-PAGE, followed by transfer to nitrocellulose, and immuno-detection with mouse monoclonal anti-hTfR2 (1:10,000), rabbit anti-TfR2 (1:10,000), anti-HA (1:2,500), H68.4 anti-TfR1 (1:5,000), sheep anti-hTfR1 (1:10,000), rabbit anti-PACS-1 (1:2,000), mouse anti-TSG101 (1:1,000), mouse anti-actin (1:10,000), mouse anti-GFP (1:2,000), rabbit anti-EGFR (1:2000), and mouse anti-μ2-AP2 (mouse mAb anti-AP50, 1:500) primary antibodies, and either HRP-conjugated or fluorescence-conjugated secondary antibodies.

RNA interference

The siRNA target sequence for PACS-1 was AACTTCAGGGCTCAAAACGT. The siRNA target sequence for TSG101 was described previously (58). The siRNA target sequence for μ2 subunit of AP-2 was AAGUGGAUGCCUUUCGGGUCA (11). All siRNAs were synthesized in Dharmacon, Inc. The siRNAs against PACS-1 or TSG101 were transfected into Hep3B/TfR2 cells using RNAiMax (Invitrogen, Carlsbad, CA) according to the reverse transfection protocol described in the manufacturer's instructions (Invitrogen, Carlsbad, CA). Briefly, 2.5 μl of 20 μM siRNA were mixed gently with 500 μl of OPTI-MEM (Invitrogen, Carlsbad, CA) in a 35-mm plate, 5 μl of RNAiMax reagent was added to the plates, mixed gently and let stand for 20 min, then 3×10^5 cells were seeded to the plates. The μ2 AP-2 was knocked down twice using RNAiMax as described above on day 1 and day 3 in HeLa/tTA-TfR2 cells.

Immunofluorescence and confocal microscopy

Cells growing on coverslips were washed twice in phosphate balanced salt solution (PBS), fixed for 15 min with 4% (vol/vol) paraformaldehyde in PBS, permeabilized for 10 min with PBS/0.5% Triton-X 100, and blocked with PBS/5%FBS for 60 min at room temperature. Cells were incubated in primary antibodies diluted into PBS/5%FBS for 30 min, washed three times for 5 min with PBS, incubated with secondary antibodies diluted in PBS for 30 min, washed five times for 5 min with PBS, and rinsed twice with distilled deionized water. Coverslips were mounted in ProLong Gold anti-fade reagent (Invitrogen, Carlsbad, CA). Images were acquired, and colocalization was quantified as described previously (6).

TfR2 was detected using the purified IgG fraction of the 16637 rabbit anti-TfR2 polyclonal anti-serum (8 μg/ml). AP-2 was detected with anti-α-AP-2 (AP.6, 1:600). Established markers of intracellular compartments were detected with various mouse monoclonal antibodies as follows: TfR1 (3B82A1 at 1.5 μg/ml), EEA1 (1:100), adaptor protein (AP)-1 (1:100). Rabbit polyclonal antibodies were detected with goat anti-rabbit Alexa Fluor 488 (1:500). Mouse monoclonal antibodies were detected with goat anti-mouse Alexa Fluor 546 (1:500).

Holo bovine Tf ^{488} and holo human Tf ^{594} (holo-Tf ^{594}) internalization

Labeling of holo-bovine Tf (Sigma-Aldrich, St. Louis, MO) with Alexa Fluor 488 was performed using Zelon Alexa Fluor 488 mouse IgG labeling kit (Invitrogen, Carlsbad, CA) according to the manufacturer's instructions. Unless specified, holo human Tf (holo-Tf) was used in experiments. HeLa/tTA-TfR2 cells transfected with scramble siRNA or μ2 AP-2 siRNA were washed twice with PBS and incubated with DMEM without FBS for 30 min at 37°C to deplete the supply of bovine-Tf available to the cells. Cells were then incubated with 300 nM holo-bovine Tf ^{488} or 20 nM holo-Tf ^{594} (Molecular Probes, Eugene, OR) at 37 °C for 20 min, washed twice with PBS, fixed, permeabilized, and stained with mouse anti-α-AP-2 antibody (1:600) and a corresponding secondary antibody as described above. TRVb cells transfected with pcDNA3-GFP-TfR2 for 48 hr were incubated with 20 nM holo-Tf ^{594} at 37°C for 20 min, washed twice with PBS, fixed and mounted with ProLong Gold anti-fade reagent.

Flow cytometry analysis

HeLa/tTA-TfR2 cells grown in the presence or absence of doxycycline (dox) (Fisher Scientific, Pittsburgh, PA) for 3 days were seeded at 5×10^4 cells/cm^2 for 24 hr., and treated with 125 μM deferoxamine for 24 hr followed by addition of 25 μM holo-Tf or holo-bovine Tf. Cells were washed twice with ice-cold PBS and detached from 10-cm dishes using cell dissociation buffer (Invitrogen, Carlsbad, CA) for 10 min at 37°C. Cells from each group were collected and aliquoted (5×10^5 cells per tube) and pelleted by centrifugation at 500 g for 5 min. For the determination of surface levels of TfR2 and TfR1, cells were incubated on ice for 90 min with a mix of either primary antibodies (25 μg/ml purified rabbit anti-TfR2 and 10 μg/ml purified mouse anti-TfR1) or IgG controls (25 μg/ml purified rabbit anti-IgG and 10 μg/ml purified mouse anti-IgG) diluted in ice-cold fluorescence-activated cell sorting staining buffer (FSB) (6,11). The cells were then washed by underlaying the cells with calf serum followed by centrifugation. For the total levels of TfR2 and TfR1, cells were fixed in fresh-diluted 4% paraformaldehyde–PBS for 15 min at room temperature, washed with cold FSB, permeabilized with NET-0.5% Triton X-100 for 10 min at 4°C, washed twice with cold FSB, incubated with primary antibodies or IgG controls described above for 30 min at 37°C, and then washed with calf serum. After incubation with the primary antibodies, cells analyzed for both surface and total TfR2/TfR1 were incubated with secondary antibodies including Alexa Fluor 488 goat anti-rabbit antibody (1:600) and goat anti-mouse R-phycoerythrin (Invitrogen, Carisbad, CA, 1:100) for 30 min on ice followed by washing

with cold calf serum. To set compensation for the TfR2 and TfR1 signals, parallel experiments were conducted. In these, the same cells as described above were incubated only with either rabbit anti-TfR2 followed by Alexa Fluor 488 goat anti-rabbit antibody or mouse anti-TfR1 followed by goat anti-mouse R-phycoerythrin incubation. The amount of surface and total TfR2/TfR1 levels were measured by fluorescence flow cytometry using a BD Biosciences FACS Calibur flow cytometer. Profiles were gated on intact single cells, based on morphology, and arithmetic mean fluorescent intensity. Unstained control and IgG controls were subtracted from all surface and total TfR2/TfR1 values for individual samples.

^{125}I-Tf uptake

Holo-Tf and holo-bovine Tf were iodinated with Na^{125}I (NEN Life Science Products) using lactoperoxidase as described previously (14). The rate of ^{125}I-holo-Tf uptake was determined as described previously (59) with the following modifications. Uptake experiments were performed on subconfluent HeLa/tTA-TfR2 cell cultures washed twice with 2 ml of MEM/20 mM HEPES, pH 7.4 and pre-treated in the same medium for 15 min in a 37 °C incubator with 5% CO_2. One milliliter of specific (MEM/20 mM HEPES, 2 mg/ml ovalbumin, and 10 nM ^{125}I-holo-Tf or 300 nM ^{125}I-holo-bovine Tf or nonspecific (specific medium with 1.25 μM holo-Tf or 3 μM holo-bovine Tf) medium was added to the appropriate cells to incubate at 37 °C with 5% CO_2 for 1 hr. After washing with PBS four times, externally bound Tf was stripped with an acidic buffer (0.5 N acetic acid, 0.5 M NaCl) for 5 min at 4 °C. Then, the cells were washed four times with 2 ml of cold final wash buffer (150 mM NaCl, 20 mM HEPES, 1 mM $CaCl_2$, 5 mM KCl, 1 mM $MgCl_2$, pH 7.4) before addition of solubilization detergent (0.1% Triton X-100, 0.1% NaOH) and counting in a gamma counter (Packard, CobraII Auto-Gamma). Surface TfR1 or TfR2 numbers were determined by counting the amount of ^{125}I-holo-Tf or ^{125}I-holo-bovine Tf bound after incubation with 10 nM ^{125}I-holo-Tf or 300 nM ^{125}I-holo-bovine Tf for 90 min on ice at 4°C. Following the 90-min incubation, the medium was removed, and cells were washed four times with 2 ml of cold final wash buffer before solubilization and counting.

Cell surface biotinylation and internalization assay

Cells transfected with siRNA for 2 days were seeded in 35-mm dish for 16 hr. Cells were washed three times with ice-cold PBS+ buffer (PBS with 0.5 mM $CaCl_2$ and 1 mM $MgCl_2$) and incubated with 0.25 mg/ml sulfosuccinimidyl-2-(biotinamido) ethyl-1,3-dithiopropionate (EZ-Link Sulfo-NHS-SS-Biotin) (Pierce, Rockford, IL) in ice-cold PBS+ for 20 min on ice. The reaction was quenched by washing the cells five times with ice-cold PBS+ buffer plus 0.1% glycine (pH 7.6). Cells were then warmed to 37°C in medium containing FBS for the desired time periods to allow internalization of the biotinylated surface components, after which they were returned to 4°C. After one rinse with NT buffer (20 mM Tris-HCl pH 8.0, 150 mM NaCl, 1 mM EDTA, and 0.2% BSA), biotin remaining at the cell surface was stripped by three 20-min incubations with ice-cold 100 mM sodium 2-mercaptoethanesulfonic acid (MesNa) (Sigma-Aldrich, St. Louis, MO) in NT. The cells were then quickly rinsed twice with NT buffer, and the residual MesNa was quenched by a 10-min incubation with ice-cold 120 mM iodoacetamide (Sigma-Aldrich, St. Louis, MO) in NT. After two additional rinses with ice-cold PBS, cells were solubilized, and cell lysate was cleared by centrifugation at 16,000 g for 5 min. Supernatants containing the internalized biotinylated proteins were pulled down with streptavidin agarose and subjected to 8% SDS-PAGE followed by immunodetection with anti-TfR2 antibody.

Supplementary Material

Refer to Web version on PubMed Central for supplementary material.

Abbreviations

TfR2	transferrin receptor 2
TfR1	transferrin receptor 1
MVB	multivesicular body
Tf	transferrin
holo-Tf	iron bound human-Tf
HeLa/tTA	HeLa cells in which expression of the transfected plasmid is controlled by the tetracycline-repressible promoter
DMEM	Dulbecco's modified Eagle's medium
MEM	Minimum Essential Medium Eagle
NET/T	NET buffer supplemented with 1% Triton X-100 and protease inhibitors
SDS-PAGE	SDS polyacrylamide gel electrophoresis
dox	doxycycline
S/T ratio	surface to total ratio
FSB	fluorescence-activated cell sorting staining buffer
PACS-1	phosphofurin acidic cluster sorting protein 1
chx	cycloheximide
EEA1	early endosome antigen 1
K	lysine
Y	tyrosine
GFP-TfR2	TfR2 with GFP fused to its N-terminus
ILV	intralumenal vesicles
DOR	delta opioid receptor.

Acknowledgments

We would like to thank Dr. Jerry Kaplan for providing anti-TSG101 antibody, TSG101 siRNA, Dr. Gary Thomas for providing PACS-1 virus and antibody, Dr. Linda Musil for providing pMT123-HA-ubiquitin, pEGFP-C1-GFPu plasmids and mouse anti-GFP antibody and Dr. Wes Sundquist for providing the plasmids of pEGFP-wt-VPS4 and pEGFP-R228Q-VPS4. We are also grateful to Dr. Gary Reiness and all members of the Enns laboratory for critical reading of the manuscript. We would like to thank Marian Morse for performing the [^{35}S] Met/Cys labeling and pulse-chase experiments. This work was supported by National Institute of Health Grant RO1-DK072166 (to C.A.E.). J.C. was partially supported by National Institutes of Health Training Grant T32 HD049309.

References

1. Gao J, Chen J, Kramer M, Tsukamoto H, Zhang AS, Enns CA. Interaction of the hereditary hemochromatosis protein HFE with transferrin receptor 2 is required for transferrin-induced hepcidin expression. Cell Metab. 2009; 9(3):217–227. [PubMed: 19254567]
2. Nemeth E, Tuttle MS, Powelson J, Vaughn MB, Donovan A, Ward DM, Ganz T, Kaplan J. Hepcidin regulates cellular iron efflux by binding to ferroportin and inducing its internalization. Science. 2004; 306(5704):2090–2093. [PubMed: 15514116]
3. Johnson MB, Enns CA. Diferric transferrin regulates transferrin receptor 2 protein stability. Blood. 2004; 104(13):4287–4293. [PubMed: 15319290]

4. Robb A, Wessling-Resnick M. Regulation of transferrin receptor 2 protein levels by transferrin. Blood. 2004; 104:4294–4299. [PubMed: 15319276]
5. Chen J, Enns CA. The Cytoplasmic domain of transferrin receptor 2 dictates its stability and response to holo-transferrin in Hep3B cells. J Biol Chem. 2007; 282(9):6201–6209. [PubMed: 17202145]
6. Johnson MB, Chen J, Murchison N, Green FA, Enns CA. Transferrin receptor 2: evidence for ligand-induced stabilization and redirection to a recycling pathway. Mol Biol Cell. 2007; 18(3): 743–754. [PubMed: 17182845]
7. Kawabata H, Tong X, Kawanami T, Wano Y, Hirose Y, Sugai S, Koeffler HP. Analyses for binding of the transferrin family of proteins to the transferrin receptor 2. Br J Haematol. 2004; 127(4):464–473. [PubMed: 15521925]
8. Ohno H, Stewart J, Fournier MC, Bosshart H, Rhee I, Miyatake S, Saito T, Gallusser A, Kirchhausen T, Bonifacino JS. Interaction of tyrosine-based sorting signals with clathrin-associated proteins. Science. 1995; 269(5232):1872–1875. [PubMed: 7569928]
9. Robb AD, Ericsson M, Wessling-Resnick M. Transferrin Receptor-2 Mediates a Biphasic Pattern of Transferrin Uptake Associated with Ligand Delivery to Multivesicular Bodies. Am J Physiol Cell Physiol. 2004
10. Watts C. Rapid endocytosis of the transferrin receptor in the absence of bound transferrin. Journal of Cell Biology. 1985; 100:633–637. [PubMed: 2857182]
11. Motley A, Bright NA, Seaman MN, Robinson MS. Clathrin-mediated endocytosis in AP-2-depleted cells. J Cell Biol. 2003; 162(5):909–918. [PubMed: 12952941]
12. Marks MS, Woodruff L, Ohno H, Bonifacino JS. Protein Targeting by Tyrosine- and Di-leucine-based Signals: Evidence for Distinct Saturable Components. Journal of Cell Biology. 1996; 135(2):341–354. [PubMed: 8896593]
13. Warren RA, Green FA, Stenberg PE, Enns CA. Distinct Saturable Pathways for the Endocytosis of Different Tyrosine Motifs. J Biol Chem. 1998; 273(27):17056–17063. [PubMed: 9642270]
14. Warren RA, Green FA, Enns CA. Saturation of the Endocytic Pathway for the Transferrin Receptor Does Not Affect the Endocytosis of the Epidermal Growth Factor Receptor. J Biol Chem. 1997; 272(4):2116–2121. [PubMed: 8999911]
15. Scott GK, Gu F, Crump CM, Thomas L, Wan L, Xiang Y, Thomas G. The phosphorylation state of an autoregulatory domain controls PACS-1-directed protein traffic. EMBO J. 2003; 22(23):6234–6244. [PubMed: 14633983]
16. Thomas C, Oates PS. IEC-6 cells are an appropriate model of intestinal iron absorption in rats. J Nutr. 2002; 132(4):680–687. [PubMed: 11925460]
17. Katzmann DJ, Odorizzi G, Emr SD. Receptor downregulation and multivesicular-body sorting. Nat Rev Mol Cell Biol. 2002; 3(12):893–905. [PubMed: 12461556]
18. Gruenberg J, Stenmark H. The biogenesis of multivesicular endosomes. Nat Rev Mol Cell Biol. 2004; 5(4):317–323. [PubMed: 15071556]
19. Hurley JH, Emr SD. The ESCRT complexes: structure and mechanism of a membrane-trafficking network. Annu Rev Biophys Biomol Struct. 2006; 35:277–298. [PubMed: 16689637]
20. Clague MJ, Urbe S. Hrs function: viruses provide the clue. Trends Cell Biol. 2003; 13(12):603–606. [PubMed: 14624836]
21. Katzmann DJ, Babst M, Emr SD. Ubiquitin-dependent sorting into the multivesicular body pathway requires the function of a conserved endosomal protein sorting complex, ESCRT-I. Cell. 2001; 106(2):145–155. [PubMed: 11511343]
22. Bache KG, Stuffers S, Malerod L, Slagsvold T, Raiborg C, Lechardeur D, Walchli S, Lukacs GL, Brech A, Stenmark H. The ESCRT-III subunit hVps24 is required for degradation but not silencing of the epidermal growth factor receptor. Mol Biol Cell. 2006; 17(6):2513–2523. [PubMed: 16554368]
23. Malerod L, Stuffers S, Brech A, Stenmark H. Vps22/EAP30 in ESCRT-II mediates endosomal sorting of growth factor and chemokine receptors destined for lysosomal degradation. Traffic. 2007; 8(11):1617–1629. [PubMed: 17714434]

24. Doyotte A, Russell MR, Hopkins CR, Woodman PG. Depletion of TSG101 forms a mammalian "Class E" compartment: a multicisternal early endosome with multiple sorting defects. J Cell Sci. 2005; 118(Pt 14):3003–3017. [PubMed: 16014378]
25. Razi M, Futter CE. Distinct roles for Tsg101 and Hrs in multivesicular body formation and inward vesiculation. Mol Biol Cell. 2006; 17(8):3469–3483. [PubMed: 16707569]
26. Theos AC, Truschel ST, Tenza D, Hurbain I, Harper DC, Berson JF, Thomas PC, Raposo G, Marks MS. A lumenal domain-dependent pathway for sorting to intralumenal vesicles of multivesicular endosomes involved in organelle morphogenesis. Dev Cell. 2006; 10(3):343–354. [PubMed: 16516837]
27. Ciechanover A, Ben-Saadon R. N-terminal ubiquitination: more protein substrates join in. Trends Cell Biol. 2004; 14(3):103–106. [PubMed: 15055197]
28. Bloom J, Amador V, Bartolini F, DeMartino G, Pagano M. Proteasome-mediated degradation of p21 via N-terminal ubiquitinylation. Cell. 2003; 115(1):71–82. [PubMed: 14532004]
29. Oestreich AJ, Aboian M, Lee J, Azmi I, Payne J, Issaka R, Davies BA, Katzmann DJ. Characterization of multiple multivesicular body sorting determinants within Sna3: 12 a role for the ubiquitin ligase Rsp5. Mol Biol Cell. 2007; 18(2):707–720. [PubMed: 17182849]
30. Watson H, Bonifacino JS. Direct binding to Rsp5p regulates ubiquitination-independent vacuolar transport of Sna3p. Mol Biol Cell. 2007; 18(5):1781–1789. [PubMed: 17332499]
31. Tait SW, de Vries E, Maas C, Keller AM, D'Santos CS, Borst J. Apoptosis induction by Bid requires unconventional ubiquitination and degradation of its N-terminal fragment. J Cell Biol. 2007; 179(7):1453–1466. [PubMed: 18166654]
32. Cadwell K, Coscoy L. Ubiquitination on nonlysine residues by a viral E3 ubiquitin ligase. Science. 2005; 309(5731):127–130. [PubMed: 15994556]
33. McNatt MW, McKittrick I, West M, Odorizzi G. Direct binding to Rsp5 mediates ubiquitin-independent sorting of Sna3 via the multivesicular body pathway. Mol Biol Cell. 2007; 18(2):697–706. [PubMed: 17182850]
34. Sipe DM, Murphy RF. Binding to cellular receptor results in increased iron release from transferrin at mildly acidic pH. J Biol Chem. 1991; 266:8002–8007. [PubMed: 2022630]
35. Bali PK, Zak O, Aisen P. A new role for the transferrin receptor in the release of iron from transferrin. Biochemistry. 1991; 30(2):324–328. [PubMed: 1988034]
36. Rutledge EA, Mikoryak CA, Draper RK. Turnover of the transferrin receptor is not influenced by removing most of the extracellular domain. J Biol Chem. 1991; 266:21125–21130. [PubMed: 1939155]
37. Rutledge EA, Root BJ, Lucas JJ, Enns CA. Elimination of the O-linked glycosylation site at Thr 104 results in the generation of a soluble human-transferrin receptor. Blood. 1994; 83(2):580–586. [PubMed: 8286753]
38. Nesterov A, Carter RE, Sorkina T, Gill GN, Sorkin A. Inhibition of the receptor-binding function of clathrin adaptor protein AP-2 by dominant-negative mutant mu2 subunit and its effects on endocytosis. EMBO J. 1999; 18(9):2489–2499. [PubMed: 10228163]
39. Calzolari A, Raggi C, Deaglio S, Sposi NM, Stafsnes M, Fecchi K, Parolini I, Malavasi F, Peschle C, Sargiacomo M, Testa U. TfR2 localizes in lipid raft domains and is released in exosomes to activate signal transduction along the MAPK pathway. J Cell Sci. 2006; 119(Pt 21):4486–4498. [PubMed: 17046995]
40. Merle U, Theilig F, Fein E, Gehrke S, Kallinowski B, Riedel HD, Bachmann S, Stremmel W, Kulaksiz H. Localization of the iron-regulatory proteins hemojuvelin and transferrin receptor 2 to the basolateral membrane domain of hepatocytes. Histochem Cell Biol. 2007; 127(2):221–226. [PubMed: 16932966]
41. Kawabata H, Germain RS, Vuong PT, Nakamaki T, Said JW, Koeffler HP. Transferrin receptor 2-alpha supports cell growth both in iron-chelated cultured cells and in vivo. J Biol Chem. 2000; 275(22):16618–16625. [PubMed: 10748106]
42. Tosoni D, Puri C, Confalonieri S, Salcini AE, De Camilli P, Tacchetti C, Di Fiore PP. TTP specifically regulates the internalization of the transferrin receptor. Cell. 2005; 123(5):875–888. [PubMed: 16325581]

43. Deinhardt K, Reversi A, Berninghausen O, Hopkins CR, Schiavo G. Neurotrophins Redirect p75NTR from a clathrin-independent to a clathrin-dependent endocytic pathway coupled to axonal transport. Traffic. 2007; 8(12):1736–1749. [PubMed: 17897318]
44. Hartung A, Bitton-Worms K, Rechtman MM, Wenzel V, Boergermann JH, Hassel S, Henis YI, Knaus P. Different routes of bone morphogenic protein (BMP) receptor endocytosis influence BMP signaling. Mol Cell Biol. 2006; 26(20):7791–7805. [PubMed: 16923969]
45. Wan L, Molloy SS, Thomas L, Liu G, Xiang Y, Rybak SL, Thomas G. PACS-1 defines a novel gene family of cytosolic sorting proteins required for trans-Golgi network localization. Cell. 1998; 94(2):205–216. [PubMed: 9695949]
46. Crump CM, Xiang Y, Thomas L, Gu F, Austin C, Tooze SA, Thomas G. PACS-1 binding to adaptors is required for acidic cluster motif-mediated protein traffic. EMBO J. 2001; 20(9):2191–2201. [PubMed: 11331585]
47. Molloy SS, Thomas L, Kamibayashi C, Mumby MC, Thomas G. Regulation of endosome sorting by a specific PP2A isoform. J Cell Biol. 1998; 142(6):1399–1411. [PubMed: 9744873]
48. Sachse M, Strous GJ, Klumperman J. ATPase-deficient hVPS4 impairs formation of internal endosomal vesicles and stabilizes bilayered clathrin coats on endosomal vacuoles. J Cell Sci. 2004; 117(Pt 9):1699–1708. [PubMed: 15075231]
49. Davies BA, Azmi IF, Katzmann DJ. Regulation of Vps4 ATPase activity by ESCRT-III. Biochem Soc Trans. 2009; 37(Pt 1):143–145. [PubMed: 19143619]
50. Aviel S, Winberg G, Massucci M, Ciechanover A. Degradation of the epstein-barr virus latent membrane protein 1 (LMP1) by the ubiquitin-proteasome pathway. Targeting via ubiquitination of the N-terminal residue. J Biol Chem. 2000; 275(31):23491–23499. [PubMed: 10807912]
51. Breitschopf K, Bengal E, Ziv T, Admon A, Ciechanover A. A novel site for ubiquitination: the N-terminal residue, and not internal lysines of MyoD, is essential for conjugation and degradation of the protein. EMBO J. 1998; 17(20):5964–5973. [PubMed: 9774340]
52. Reinstein E, Scheffner M, Oren M, Ciechanover A, Schwartz A. Degradation of the E7 human papillomavirus oncoprotein by the ubiquitin-proteasome system: targeting via ubiquitination of the N-terminal residue. Oncogene. 2000; 19(51):5944–5950. [PubMed: 11127826]
53. Hislop JN, Marley A, Von Zastrow M. Role of mammalian vacuolar protein-sorting proteins in endocytic trafficking of a non-ubiquitinated G protein-coupled receptor to lysosomes. J Biol Chem. 2004; 279(21):22522–22531. [PubMed: 15024011]
54. Reggiori F, Pelham HR. Sorting of proteins into multivesicular bodies: ubiquitin-dependent and -independent targeting. EMBO J. 2001; 20(18):5176–5186. [PubMed: 11566881]
55. Vogt T, Blackwell A, Giannetti A, Bjorkman P, Enns C. Heterotypic interactions between transferrin receptor and transferrin receptor 2. Blood. 2002; 101(5):2008–2014. [PubMed: 12406888]
56. Scott GK, Fei H, Thomas L, Medigeshi GR, Thomas G. A PACS-1, GGA3 and CK2 complex regulates CI-MPR trafficking. EMBO J. 2006; 25(19):4423–4435. [PubMed: 16977309]
57. Laemmli UK. Cleavage of structural proteins during the assembly of the head of bacteriophage T4. Nature. 1970; 227:680–685. [PubMed: 5432063]
58. Garrus JE, von Schwedler UK, Pornillos OW, Morham SG, Zavitz KH, Wang HE, Wettstein DA, Stray KM, Cote M, Rich RL, Myszka DG, Sundquist WI. Tsg101 and the vacuolar protein sorting pathway are essential for HIV-1 budding. Cell. 2001; 107(1):55–65. [PubMed: 11595185]
59. Roy CN, Penny DM, Feder JN, Enns CA. The hereditary hemochromatosis protein, HFE, specifically regulates transferrin-mediated iron uptake in HeLa cells. J Biol Chem. 1999; 274(13): 9022–9028. [PubMed: 10085150]

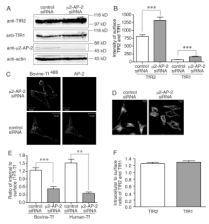

Figure 1.

TfR2 endocytosis requires AP-2. A) Total TfR2 and TfR1 levels in response to knockdown of μ2 AP-2. HeLa/tTA-TfR2 cells were knocked-down twice with control siRNA or μ2 AP-2 specific siRNA (once on day 1 and once on day 3). On day 5, cells were lysed and subjected to 10% SDS-PAGE. Proteins of interest were immuno-detected with anti-TfR2, anti-TfR1, anti-μ2 AP-2, and anti-actin antibodies, or subjected to the analysis described in panels B, C, D, and E. B) Surface levels of TfR2 and TfR1 increase in AP-2-depleted cells. Control and AP-2-depleted HeLa/tTA-TfR2 cells were incubated with rabbit anti-TfR2 and mouse anti-TfR1 for 90 min at 4°C, and then incubated with corresponding secondary antibodies followed by flow cytometry analysis as described in Materials and Methods. C) Depletion of AP-2 blocks uptake of bovine-Tf488. Control and AP-2-depleted HeLa/tTA-TfR2 cells were incubated with DMEM without serum for 15 min prior to incubation with bovine-Tf^{488} for 30 min. The cells were fixed, permeabilized and incubated with anti-α AP-2 antibody followed by incubation with rabbit anti-mouse Alexa Fluor 546 antibody. Scale bar represents 10 μm. D) Depletion of AP-2 blocks uptake of holo-Tf^{594}. Control and AP-2-depleted HeLa/tTA-TfR2 cells with addition of dox to turn of TfR2 expression were incubated with DMEM without serum for 15 min prior to incubation with holo-Tf^{594} for 30 min, and then fixed for image analysis. Scale bar represents 10 μm. E) Depletion of AP-2 blocks uptake of holo-bovine ^{125}I-Tf and holo-^{125}I-Tf. Control and AP-2-depleted HeLa/tTA-TfR2 cells in 100-mm plates, were split to 6-well plates on day 5 with 4×10^5 cells per well. Holo-^{125}I-Tf and holo-bovine ^{125}I-Tf uptake was performed on the next day as described in Materials and Methods. F) The intracellular to surface ratio of TfR2 and TfR1 are 1.27 and 1.30, respectively, in static state. The average intracellular to surface ratio of TfR2 and TfR1 were calculated from the surface and total levels of TfR2 and TfR1 measured by flow cytometry analysis in B. These experiments were repeated at least twice with similar results. Data were evaluated by Student's t test; p-values < 0.001 are indicated by *** and < 0.01 by **, respectively.

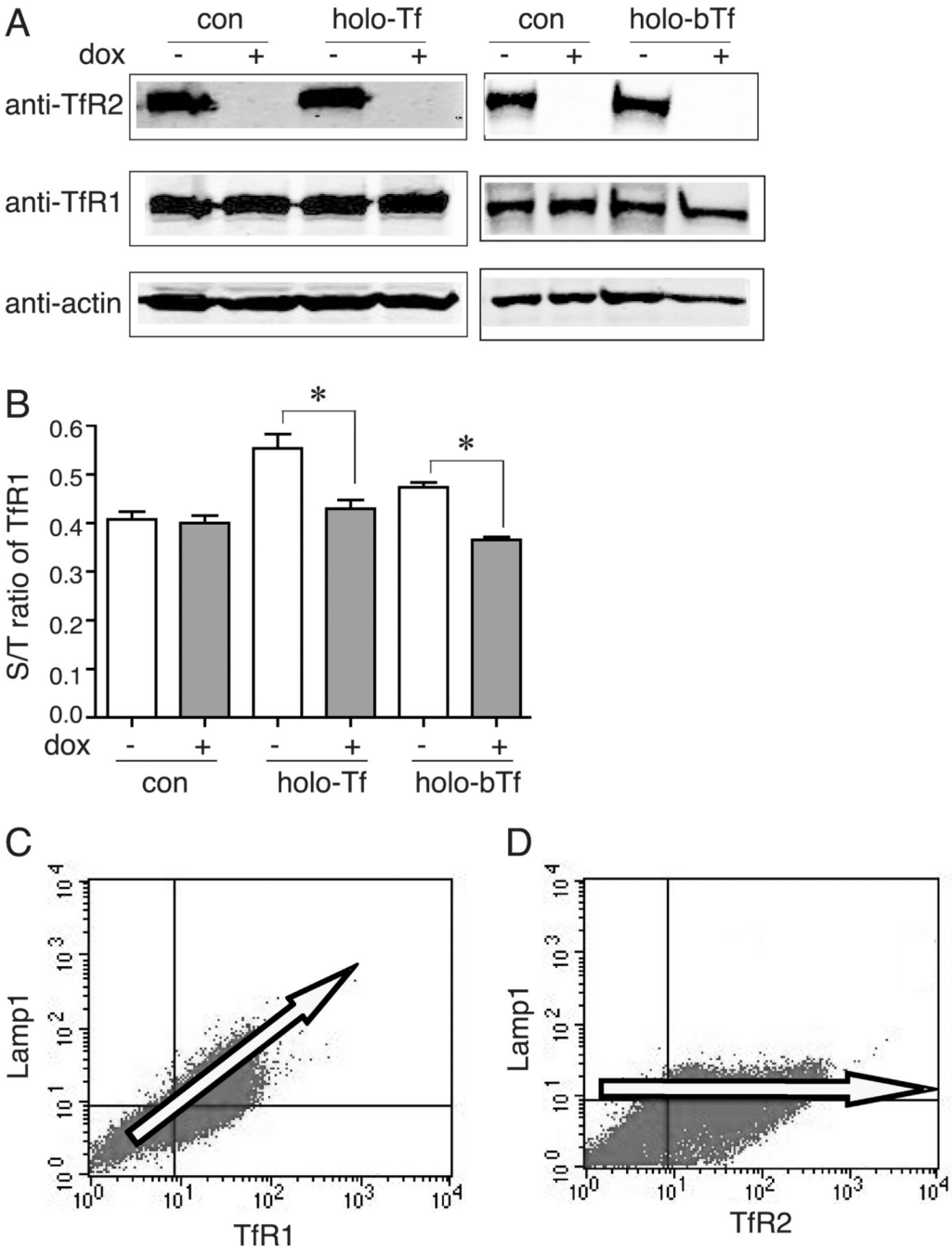

Figure 2.

TfR2 and TfR1 compete for endocytosis only in the presence of holo-Tf. A) Total TfR1 levels are constant in HeLa/tTA-TfR2 cells in the presence of deferoxamine regardless of the presence of Tf or dox in the media, and TfR2 was turned off by adding dox. HeLa/tTA-TfR2 cells in the presence or absence of dox were treated with 150 μM deferoxamine for 24 hr prior to treatment with 25 μM holo-Tf or holo-bovine Tf (holo-bTf) for 30 min. Cell lysates were analyzed by immunoblot with anti-TfR2, anti-TfR1, and anti-actin antibodies. B) Lack of competition between TfR2 and TfR1 for endocytosis in absence of holo-Tf in contrast to competition of TfR1 with TfR2 in presence of holo-Tf in HeLa/tTA-TfR2 cells. HeLa/tTA-TfR2 cells in absence or presence of TfR2 were treated without or with 25 μM

holo-Tf or holo-bTf for 30 min. Surface and total levels of TfR1 and TfR2 were measured by flow cytometry analysis as described in *Materials and Methods*. Data were evaluated by Student's t test; p-values < 0.05 are indicated by *. C) TfR1 competes with Lamp1 for endocytosis. Surface TfR1 and Lamp1 levels were analyzed in absence of dox in HeLa/TfR1 20-2 cells by flow cytometry analysis. D) Lack of competition of TfR2 with Lamp1 for endocytosis. Surface TfR2 and Lamp1 levels were analyzed by flow cytometry analysis in the HeLa/TfR1 20-2 cells transiently transfected with TfR2 when TfR1 was turned off by the addition of dox. These experiments were repeated at least twice with similar results.

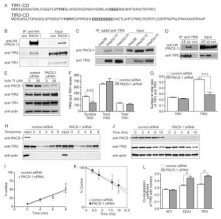

Figure 3.

TfR2 recycles to the cell surface by interacting with PACS-1. A) Sequence of the cytoplasmic domain (CD) of TfR2 and TfR1. Acidic cluster motifs (underlined) and endocytic motifs are marked in bold. B) PACS-1-HA interacts with TfR2 but not with TfR1. Hep3B/TfR2 cells were infected with PACS-1-HA adenovirus/Trans adenovirus (PACS-1) or Trans adenovirus (con) for 48 hr. Cell lysates were immunoprecipitated with anti-HA antibody. The immunoprecipitated proteins were immunodetected with rabbit anti-TfR2, mouse anti-HA and mouse anti-TfR1 (3B82A1) antibodies. C) Holo-Tf does not abrogate the interaction between endogenous TfR2 and endogenous PACS-1 in HepG2 cells. HepG2 cells were treated with 25 μM holo-Tf for 24 hr. Cell lysates were immunoprecipitated with rabbit anti-TfR2 antibody followed by immunoblot with mouse anti-TfR2 and rabbit anti-PACS-1 antibodies. Hep3B cells that do not express TfR2 were used as a negative control. D) The acid cluster motif in the cytoplasmic domain of TfR2 is required for the interaction between TfR2 and PACS-1. Hep3B/ΔE-TfR2 (ΔE) and Hep3B/TfR2 (wt) cells were infected and immunoprecipitated as described in A. Hep3B/ΔE-TfR2 cells infected with Trans adenovirus was used as a control (con). E) Depletion of PACS-1 by siRNA does not affect the total levels of TfR2 and TfR1 and the response of TfR2 to holo-Tf. Hep3B/TfR2 cells in 60-mm plates were transfected with control or PACS-1 specific siRNA for 32 hr, and then split into two 35-mm plates for overnight, and treated with 25 μM holo-Tf for 24 hr followed by immuno-detection with anti-PACS-1, anti-TfR2, anti-TfR1 and anti-actin antibodies. F, G) Depletion of PACS-1 decreases surface TfR2 levels (G) and the S/T ratio of TfR2 (H), but did not alter S/T ratio (H) and total levels (G) of TfR1. Surface and total levels of TfR1 and TfR2 were measured in control and siRNA-treated Hep3B/TfR2 cells by flow cytometry. H) Knockdown of PACS-1 does not affect degradation rate of TfR2. Control and PACS-1-depleted Hep3B/TfR2 cells were treated with 100 μg/ml chx for 0, 2, 4, 8, or 12 hr. Cell lysates were analyzed by immunoblot for PACS-1, TfR2 and actin using fluorescent secondary antibodies. One representative of three independent experiments is shown. I) Quantitation of TfR2 degradation in Hep3B/TfR2 cells. The levels of TfR2 were normalized to actin, and TfR2 level treated with chx for 0 h was set as 100%. The average data from two independent experiments were presented. J) Depletion of PACS-1 does not alter internalization of TfR2. Surface TfR2 was biotinylated followed by internalization, streptavidin pull down and immunoblot as described in *Materials and Methods*. 10% of total input (input) was run in parallel in 9% SDS-PAGE. One representative of two independent experiments is shown. K) Quantitation of TfR2 internalization. Internalized TfR2 was normalized to surface TfR2 (0 min) and set as 100%. The rate of internalization was determined by linear regression analysis. The average data from three independent experiments were shown. L) Depletion of PACS-1 increases co-localization of TfR2 with EEA1 and TfR1 markers, but it did not affect co-localization of TfR2 with AP-1. Co-localization of TfR2 with EEA1, TfR1 and AP-1 was quantified from at least 60 cells in three independent experiments and analyzed as described in *Materials and Methods*. The experiments in A–F were repeated at least twice with similar results. Data were evaluated by Student's t test; p-values < 0.05, < 0.01 and < 0.001 are indicated by *, ** and ***, respectively.

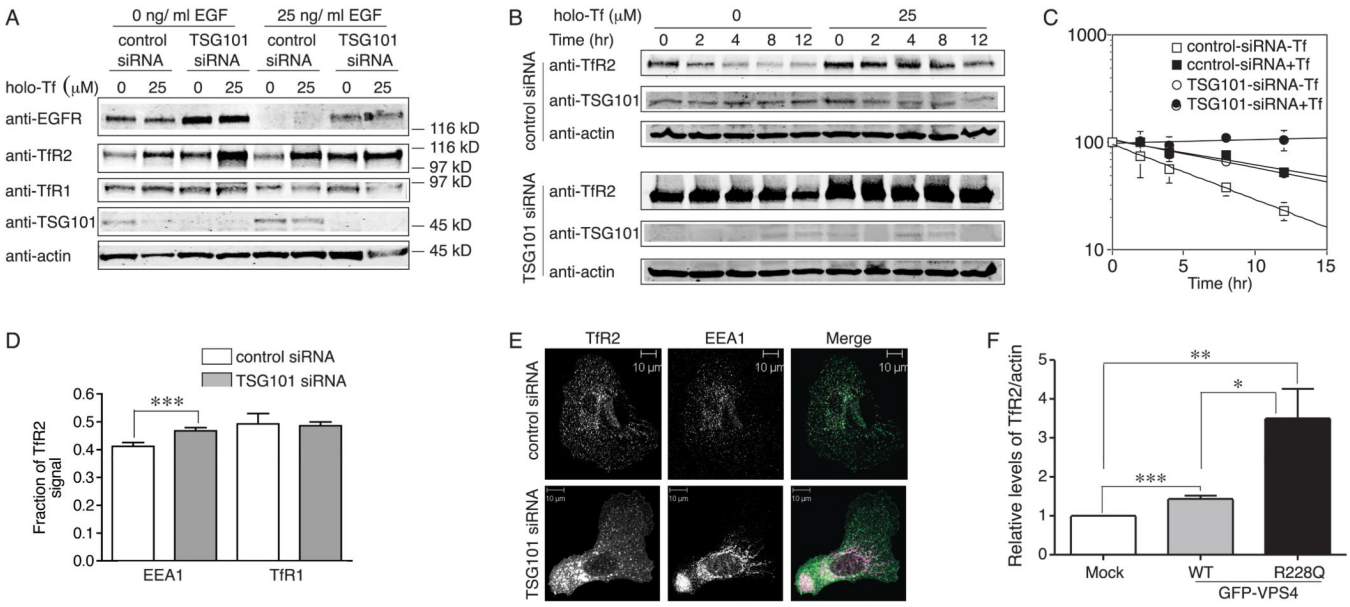

Figure 4.

TfR2 is most likely degraded in the lysosome through the MVB pathway. A) Knockdown of TSG101 increases the levels of TfR2 and EGFR. Hep3B/TfR2 cells in 60-mm plates were transfected with control or TSG101 specific siRNA for 32 hr, and then split into four 35-mm plates, and treated with 25 μM holo-Tf for 24 hr followed by serum starvation overnight. Cell lysates were subjected to 10% SDS-PAGE and immunoblot with anti-EGFR, anti-TfR2, anti-TSG101 and anti-actin antibodies. One representative blot of three independent experiments is shown. B) Knockdown of TSG101 blocks degradation of TfR2. Control and TSG101-depleted cells were treated and analyzed as described in Figure 3. One representative of three independent experiments is shown. C) Quantitation of TfR2 degradation. The average data from two independent experiments were analyzed and presented as described in Figure3. The average data from two independent experiments were analyzed as described in Figure 3. D) Knockdown of TSG101 increases the fraction of TfR2 co-localizing with EEA1 by 20%. Co-localization of TfR2 with EEA1 and TfR1 was quantified from at least 30 cells and analyzed as described in *Materials and Methods*. Data were evaluated by Student's t test; p-value < 0.001 is indicated by ***. E) Knockdown of TSG101 alters the morphology of the early endosome. The morphology of control and TSG101-depleted Hep3B/TfR2 cells was examined by immunofluorescence microscopy with rabbit anti-TfR2 and mouse anti-EEA1 antibodies as described in *Materials and Methods*. Early endosomes in TSG101-depleted cells formed tubular structures whereas they appeared as a punctate pattern in control cells. F) Dominant negative Vps4 inhibits degradation of TfR2. Hep3B/TfR2 cells in 35-mm plates were transiently transfected with pEGFP-wt-VPS4 and pEGFP-R228Q-Vps4 or empty vector as described *Materials and Methods*. Cell lysate were subjected to 10% SDS-PAGE and immunoblot with anti-TfR2, anti-GFP and anti-actin antiboies. The levels of TfR2 were normalized to actin, and the normalized to mock transfection cells. The average data from four independent experiments was shown. Data were evaluated by Student's t test; p-values < 0.001, < 0.01 and < 0.1 are indicated by ***, ** and * respectively.

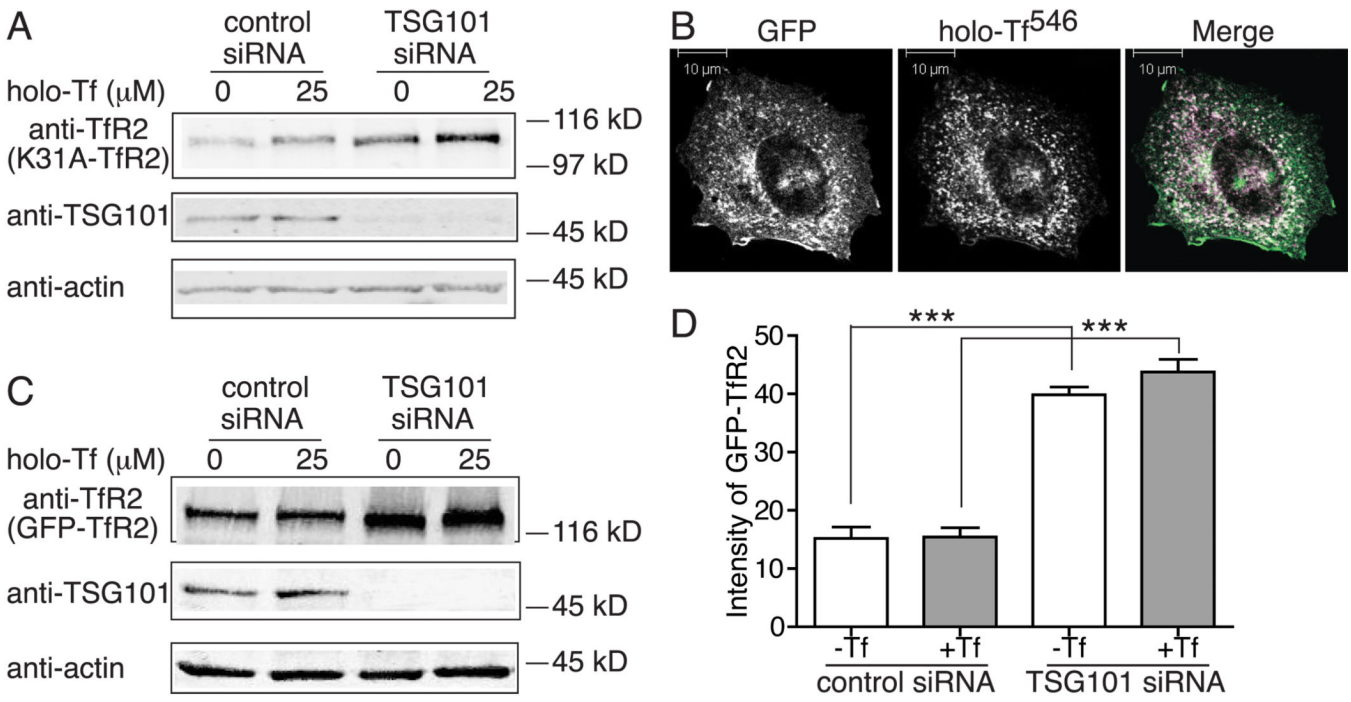

Figure 5.

TfR2 degradation is not ubiquitination-dependent. A) Knockdown of TSG101 blocks degradation of K31A-TfR2. Hep3B/K31A-TfR2 cells in 35-mm plates were transfected with control or TSG101 specific siRNA for 32 hr and then split to two 35-mm plates for overnight and treated with holo-Tf for 24 hr. Cell lysates were subjected to 10% SDS-PAGE and immunodetection with anti-TfR2, anti-TSG101 and anti-actin antibodies. This experiment was repeated once with the same results. B) GFP-TfR2 internalizes in TRVb cells. GFP-TfR2 was transfected in TRVb cells, and holo-Tf^{546} uptake was performed at 37°C for 20 min followed by confocal microscopy. Scale bar represents 10 μm. C) Knockdown of TSG101 increases the level of GFP-TfR2. Hep3B/GFP-TfR2 cells were transfected, treated and analyzed as described in A. D) Knockdown of TSG101 increases the level of GFP-TfR2 by flow cytometry analysis. Hep3B/GFP-TfR2 cells were transfected and treated as described in A, and GFP-TfR2 levels were measured by flow cytometry. Hep3B cells that do not express GFP-TfR2 were used as a control. The control was subtracted from the Hep3B-GFP-TfR2 cells. The experiments were performed in quadruplicate. The average data from two independents were shown in D. Data were evaluated by Student's t test; p-value < 0.001 is indicated by ***.